Toward the Discovery of New Elements: Production of Livermorium (Z=116) with ^{50}Ti

Gates, J. M.; Orford, R.; Rudolph, D.; Appleton, C.; Barrios, B. M.; Benitez, J. Y.; Bordeau, M.; Botha, W.; Campbell, C. M.; Chadderton, J.; Chemey, A. T.; Clark, R. M.; Crawford, H. L.; Despotopulos, J. D.; Dorvaux, O.; Esker, N. E.; Fallon, P.; Folden, C. M.; Gall, B. J. P.; Garcia, F. H.; Golubev, P.; Gooding, J. A.; Grebo, M.; Gregorich, K. E.; Guerrero, M. ; Henderson, R. A.; Herzberg, R. -D.; Hrabar, Y.; King, T. T.; Kireeff Covo, M.; Kirkland, A. S.; Krücken, R.; Leistenschneider, E.; Lykiardopoulou, E. M.; McCarthy, M.; Mildon, J. A.; Müller-Gatermann, C.; Phair, L.; Pore, J. L.; Rice, E.; Rykaczewski, K. P.; Sammis, B. N.; Sarmiento, L. G.; Seweryniak, D; Sharp, D. K.; Sinjari, A.; Steinegger, P.; Stoyer, M. A.; Szornel, J. M.; Thomas, K.

Published in:
Physical Review Letters

DOI:
10.1103/PhysRevLett.133.172502

2024

Document Version:
Publisher's PDF, also known as Version of record

Supplemental Material
Towards the Discovery of New Elements: Production of Livermorium ($Z = 116$) with ^{50}Ti

The Supplemental Material provides (i) detailed results and statistical assessments in the analysis of events stemming from decay chains starting with the isotope ^{290}Lv, and (ii) details concerning the search parameters for decay chains originating from ^{291}Lv.

The numbering of references in this Supplemental Material corresponds to references in the main article.

I. DETAILS OF PUBLISHED ^{290}LV DECAY CHAINS

Decay properties such as decay energies and lifetimes, relating to various ensembles of data associated with previous experiments in the direct or indirect production of ^{290}Lv, ^{286}Fl, or ^{282}Cn, and with the result of the present work (cf. main article) included, are compiled: Distributions of decay energies and correlation times along with determined E_α and $T_{1/2}$ values are presented for the different ensembles in Fig. 1 for ^{286}Fl and ^{282}Cn, respectively. An overview, together with a statistical assessment of the correlation times attributed to the single decay steps relevant to the current study, is presented Table I for the ensembles of decay chains corresponding to ^{290}Lv (cf. main article) and Fig. 1, respectively. Table II provides a summary of aggregated experimental results concerning the decays of ^{290}Lv, ^{286}Fl, and ^{282}Cn.

II. SEARCH PARAMETERS FOR DECAY CHAINS ORIGINATING FROM ^{291}LV

The known decay chain originating from ^{291}Lv and its daughters typically terminates in spontaneous fission (SF) at ^{283}Cn or ^{279}Ds, although it has been observed to decay via emission of α particles to the SF-decaying ^{267}Rf [63-69,71]. Candidates for decay chains originating from this isotope were searched for by looking for correlations, required to all be detected within the same pixel of the detector, that consisted of an:

1. Evaporation residue (EVR) [$10 < E\,(\mathrm{MeV}) < 30$] followed by at least one α-like particle [$9.50 < E\,(\mathrm{MeV}) < 11.25$] within 3 s, followed by a spontaneous fission-like event with $E > 120$ MeV within 25 s.

2. EVR [$10 < E\,(\mathrm{MeV}) < 30$] followed by at least two α-like particles [$9.00 < E\,(\mathrm{MeV}) < 11.25$] within 30 s, followed by a spontaneous fission-like event with $E > 120$ MeV within 2 s.

3. EVR [$10 < E\,(\mathrm{MeV}) < 30$] followed by three or more α-like particles [$8.00 < E\,(\mathrm{MeV}) < 11.25$] within 300 s, followed by a spontaneous fission-like event with $E > 120$ MeV within 150 min.

These α-particle energy ranges were chosen to fully encompass the known energy ranges for chains terminating in SF at ^{283}Cn, ^{279}Ds, and ^{267}Rf, respectively. The lifetimes were chosen to accept events within five half-lives of known decays. The efficiency for detecting a decay chain originating from ^{291}Lv under these conditions is $\approx 85\%$. The probability for any one of the SF-like events to combine with random background-like events to form a chain meeting the requirements listed above is 1.4×10^{-3}, 2.1×10^{-6}, and 1.7×10^{-3}, for conditions (1)-(3), respectively. If a chain is observed within these broad parameters, then lifetimes and decay energies must also fall within accepted windows for the known isotopes, thus reducing random rates further.

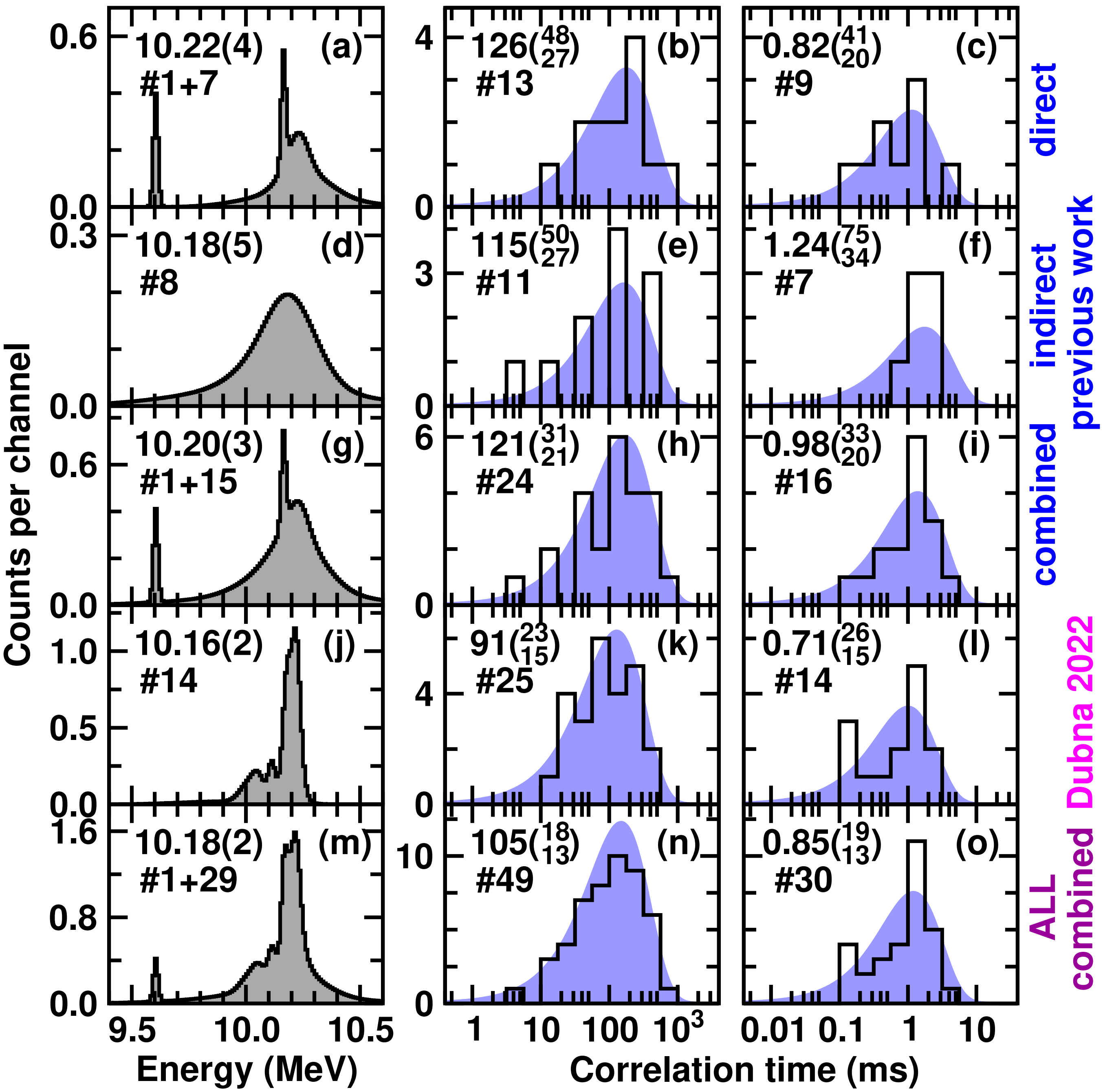

FIG. 1: (Color online) The left column provides experimental decay-energy spectra from events associated with the decay step ^{286}Fl$\rightarrow$ ^{282}Cn. For a single entry, a Gaussian with integral one and a width compliant with its measured uncertainty was added into the respective spectrum. The numbers at the top left of each panel in the left column are the (α-decay) energies extracted by computing the histogram mean in the interval [9.9,10.5] MeV. The middle and right columns provide the correlation times for the decays of ^{286}Fl and ^{282}Cn, respectively. Experimental data points are comprised in the histograms (black lines). The shaded areas (blue) provide correlation-time distributions expected for the corresponding half life, $T_{1/2}$, which are given in the top left corner of each panel. For all panels, the number behind the hashtag, #, indicates the number of available data points. The first row, panels (a)-(c), refers to previous direct production of ^{286}Fl [14,66-68]. The second row, panels (d)-(f), refers to previous indirect production of ^{286}Fl [64,65,71]. The spectra in the third row, panels (g)-(i), are the sums of the spectra in the first and second row. The fourth row, panels (j)-(l), refer to the recent data obtained at JINR Dubna [69]. The spectra in the fifth row, panels (m)-(o), are the sums of the spectra in the third and fourth row, i.e. comprise current best values for the main decay characteristics of ^{286}Fl and ^{282}Cn prior to the present study. For the update *including* the data points from the present study, see Fig. 2 of the main article and Table I of this Supplemental Material. For the interpretation of the peak at 9.60(1) MeV in panels (a), (g), and (m), see Refs. [14,72].

TABLE I: Overview of correlation time analyses of single decay steps according to Ref. [74] of various ensembles of decay chains associated with previous direct ('Cn&Fl') and indirect ('Lv&Og') production of ^{286}Fl, recent production of ^{286}Fl [69], and the present events interpreted to start from ^{290}Lv, respectively. These correspond to ensembles as displayed in the respective rows of Fig. 3 in the main article and Fig. 1.

Label	previous (Cn&Fl)	previous (Lv&Og)	previous	^{286}Fl (2022)	all	including this work
References	[14,66-68]	[64,65,71]		[69]		
^{290}Lv						
No. of chains		16	16		16	18
data points		11	11		11	13
$T_{1/2}(^{290}\text{Lv})$ (ms)		$8.3(^{36}_{19})$	$8.3(^{36}_{19})$		$8.3(^{36}_{19})$	$8.2(^{32}_{18})$
$\sigma_{\Theta_{\text{exp}}}$		2.13^b	2.13^b		2.13^b	2.02^b
$[\sigma_{\Theta,\text{low}}, \sigma_{\Theta,\text{high}}]$ [74]		[0.67,1.81]	[0.67,1.81]		[0.67,1.81]	[0.72,1.77]
data points		11	11		11	12
E_{decay} (MeV)		10.84(8)	10.84(8)		10.84(8)	$10.84(7)^a$
^{286}Fl						
No. of chains	13	16	29	25	54	56
data points	13	11	24	25	49	51
$T_{1/2}(^{286}\text{Fl})$ (ms)	$126(^{48}_{27})$	$115(^{57}_{31})$	$121(^{31}_{21})$	$91(^{23}_{15})$	$105(^{18}_{13})$	$106(^{17}_{13})$
$\sigma_{\Theta_{\text{exp}}}$	0.96	1.44	1.22	0.97	1.10	1.11
$[\sigma_{\Theta,\text{low}}, \sigma_{\Theta,\text{high}}]$ [74]	[0.72,1.77]	[0.67,1.81]	[0.84,1.72]	[0.85,1.71]	[0.97,1.57]	[0.98,1.58]
data points	7	8	15	14	29	31
E_{decay} (MeV)	10.22(4)	10.18(5)	10.20(3)	10.16(2)	10.18(2)	$10.18(2)^c$
^{282}Cn						
data points	9	7	16	14	30	32
$T_{1/2}(^{282}\text{Cn})$ (ms)	$0.82(^{41}_{20})$	$1.24(^{75}_{34})$	$0.98(^{33}_{20})$	$0.71(^{26}_{15})$	$0.85(^{19}_{13})$	$0.88(^{19}_{13})$
$\sigma_{\Theta_{\text{exp}}}$	0.99	0.43^d	0.87	1.04	0.98	0.97
$[\sigma_{\Theta,\text{low}}, \sigma_{\Theta,\text{high}}]$ [74]	[0.62,1.84]	[0.52,1.87]	[0.77,1.75]	[0.73,1.77]	[0.89,1.67]	[0.90,1.66]

[a]Result from the integration of the energy spectrum in Fig. 3(a) of the main article in the interval [10.0,11.7] MeV.
[b]The experimental value for $\sigma_{\Theta_{\text{exp}}}$ falls outside the upper 1-σ confidence limit [74].
[c]Result from the integration of the energy spectra in the left column of Fig. 1 in the interval [9.9,10.5] MeV.
[d]The experimental value for $\sigma_{\Theta_{\text{exp}}}$ falls outside the lower 1-σ confidence limit [74].

TABLE II: Summary of aggregated experimental results concerning the decays of ^{290}Lv, ^{286}Fl, and ^{282}Cn.

	E_α (MeV)	Q_α (MeV)	$T_{1/2}$ (ms)	b_α [a]	$T_{1/2}(\alpha)$ [b] (ms)	HF [b]	$T_{1/2}(\text{SF})$ [b] (ms)
^{290}Lv	10.84(7)	10.99(7)	$8.2(^{32}_{18})$	1	$8.2(^{32}_{18})$	$1.4(^{15}_{7})$	not applicable
^{286}Fl	10.18(2)	10.32(2)	$106(^{17}_{13})$	31/56	$191(^{31}_{23})$	$2.2(^{7}_{5})$	$247(^{40}_{30})$
	$9.57(3)^c$	9.71(3)		1/56	$5.9(^{10}_{7}) \times 10^3$	$1.3(^{5}_{4})$	
^{282}Cn	not applicable		$0.88(^{19}_{13})$	0	not applicable		$0.88(^{19}_{13})$

[a]Due to incomplete knowledge from some previous studies, the branching ratio can only be estimated.
[b]The uncertainties cannot account for uncertainties in branching ratios. See preceding note. Hindrance factors were calculated based on C. Qi *et al.*, Phys. Rev. C 80, 044326 (2009). See also Refs. [14,72].
[c]See corresponding note in Table II in Ref. [14].